Journal of Molecular Structure 1176 (2019) 703–710

Contents lists available at ScienceDirect

Journal of Molecular Structure

journal homepage: http://www.elsevier.com/locate/molstruc

Crystal structure of {N-(2-hydroxyethylamino)ethylsalicylaldiminato]-palladium(II) chloride}: Synthesis, X-ray structure, electrochemistry, DFT and TDDFT studies

Ali Hasnaoui [a], Ismail Hdoufane [b], Rachid Idouhli [c], Bruno Therrien [d], Mustapha Ait Ali [a], Larbi El Firdoussi [a], *

[a] *Équipe de Chimie de Coordination et Catalyse, Université Cadi Ayyad, Faculté des Sciences Semlalia, BP 2390, Marrakech, Morocco*
[b] *Laboratoire de Chimie Moléculaire, Université Cadi Ayyad, Faculté des Sciences Semlalia, BP 2390, Marrakech, Morocco*
[c] *Physical-Chemistry of Materials and Environment Laboratory, Faculty of Sciences Semlalia, Cadi Ayyad University, Marrakech, Morocco*
[d] *Neuchâtel Platform of Analytical Chemistry, Institute of Chemistry, University of Neuchâtel, Avenue de Bellevaux 51, CH-2000 Neuchâtel, Switzerland*

ARTICLE INFO

Article history:
Received 19 June 2018
Received in revised form
30 August 2018
Accepted 31 August 2018
Available online 11 September 2018

Keywords:
Schiff base
Palladium complex
X-ray structure
Electrochemistry
DFT
TDDFT

ABSTRACT

A new complex N-(2-hydroxyethylamino)ethylsalicylaldiminato]-palladium(II) chloride [Pd(L)Cl] was synthesized by the reaction in ethanol of the Schiff base 2-(2-(2-hydroxyethylamino)ethylimino)methyl phenol (LH) and Li_2PdCl_4. The complex was characterized by ^{1}H NMR, ^{13}C NMR, FT-IR and UV–Vis spectroscopic techniques. The structure of the complex was confirmed by single-crystal X-ray structure analysis. The electrochemical properties of $PdCl_2$ and [Pd(L)Cl] have been investigated by cyclic voltammetry. Additionally, the electronic structure, the solution spectrum and the redox property of [Pd(L)Cl] have been rationalized by DFT and TDDFT methods.

1. Introduction

Palladium complexes have gained a huge interest in synthetic, pharmaceutical and material chemistry and their applications in C–C and C–N cross-coupling reactions make them very popular for the preparation of versatile organic building blocks [1–6]. Palladium is relatively non-toxic, and some palladium complexes can be handled under air [7], in supported form [8], in ionic liquid medium as well as in water [9]. These aspects are particularly important for industries and contribute to the development of environmentally-friendly chemical processes.

The use of Schiff base ligands in inorganic, biological and analytical chemistry has been extensively studied [10]. Schiff bases play an important role as organic ligands in coordination chemistry, because they can easily coordinate transition metals to form stable complexes [11,12]. Numerous reports have shown prominent biological properties of Schiff base complexes [13], especially due to the presence of an imine group in the ligand [14–16]. Moreover, it is well known that metal complexes having N,O donors exhibit interesting biological activities such as anticancer [17], antifungal [18] and antibacterial [19,20]. Furthermore, such complexes play a major role in developing the coordination chemistry related to catalysis, enzymatic reaction, electrochemistry, magnetism and bioinorganic modeling studies [21–23].

Among the multitude of Schiff base ligands, the 2-(2-(2-hydroxyethylamino)ethylimino)methyl phenol (LH) was first coordinated to metals in the 1970s [24]. This versatile ligand possesses four coordination sites of different reactivity (see Scheme 1), thus forming according to the reaction conditions and the transition metal used, complexes of variable denticity [25–28]. Therefore, in view to contribute to the finding of new complexes that could be valuable for the oxidation of natural terpenic olefins using electrochemical methods, we report here the synthesis of a water-stable Schiff base N,N,O palladium(II) complex [Pd(L)Cl]. The complex was characterized by different spectroscopic techniques and its molecular structure was confirmed by single-crystal X-ray

---

* Corresponding author.
E-mail address: elfirdoussi@uca.ac.ma (L. El Firdoussi).

https://doi.org/10.1016/j.molstruc.2018.08.111

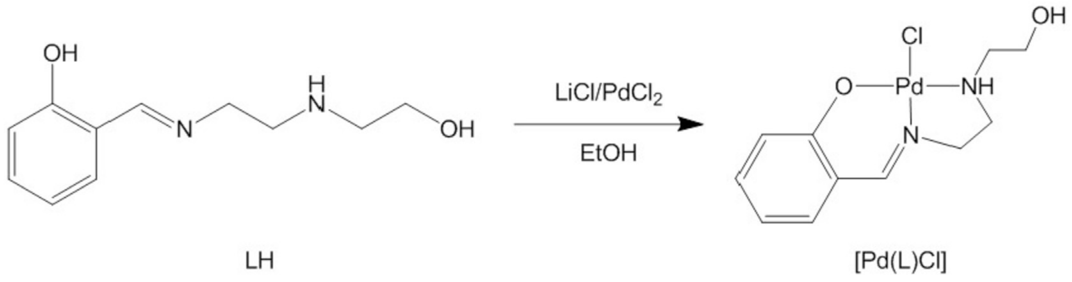

Scheme 1. Synthesis of [Pd(L)Cl].

structure analysis. Theoretical analysis of the geometries and electronic properties of the complex was studied using DFT and TDDFT methods, while, the redox properties of $PdCl_2$ and [Pd(L)Cl] were investigated by cyclic voltammetry.

2. Experimental

2.1. Material and methods

$PdCl_2$, LiCl, ethanol, 2-hydroxyethylamine and salicylaldehyde were purchased from Sigma Aldrich. The ligand 2-(2-(2-hydroxyethylamino)ethylimino)methyl phenol (LH) has been prepared by the condensation of salicylaldehyde and 2-hydroxyethylamine as described in the literature [29]. [Pd(L)Cl] was synthesized by a procedure adapted from our previous work [30]. NMR studies were recorded in DMSO-d_6 using a Bruker Avance 300 spectrometer. Chemical shifts are given in ppm relative to external TMS and coupling constants (*J*) are provided in Hz. FT-IR analysis was performed on a VERTEX 70 in KBr and the UV–vis 2550 Shimadzo spectra were recorded at room temperature in the range of 200–900 nm. For MS detection, the ionization was performed on a 4000 QTrap (AB SciexTM) in positive ESI mode using a mass scan range of 200–550 Da. Experimental source parameters were as follows: ion spray voltage 5500 V, ion source gas GS1 30 psi, curtain gas CUR 10 psi and declustering potential 80 V. The sample was dissolved in methanol (HPLC grade), at 1 μg/mL, and injected in the Turbo VTM ion source by a syringe pump (Harvard Apparatus, USA) with a flow rate of 20 μL/min. Cyclic voltammetry measurements were realized using a potentiostat PGZ100 equipped with a standard three-electrode configuration. A platinum wire working electrode, a platinum mesh auxiliary electrode and Ag/AgCl (saturated KCl) reference electrode. Voltammetry measurements were carried out in distillate water/ethanol (50/50: v/v) solution with 2 mM nitrate potassium as the supporting electrolyte.

2.2. Synthesis of [Pd(L)Cl]

A mixture of $PdCl_2$ (43 mg, 0.24 mmol) and LiCl (30 mg, 0.7 mmol) in 20 mL of ethanol was stirred at 60 °C until the appearance of a light orange color. Then, the LH ligand (0.015 g, 0.07 mmol) was added at room temperature. After 2 h, a yellow precipitate was observed. The solid was filtered and washed with ethanol. Recrystallization from ethanol afforded the product, [Pd(L)Cl] in 53% yield (0.013 g, 0.037 mmol).

$C_{11}H_{15}ClN_2O_2Pd$ Color yellow: ESI-MS (positive mode) $m/z = 313.3$ $[M\text{-}Cl]^+$. FT-IR (cm^{-1}, KBr): υ(C=N) 1635, υ(C–O) 763. ^1H NMR (300 MHz, DMSO-d_6, ppm): 3.20–3.80 (6H, m), 3.91 (1H, m), 4.81 (1H, t, *J* = 5.2 Hz), 5.93 (1H, S), 6.53 (1H, t, *J* = 7.3 Hz), 6.72 (1H, d, *J* = 8.4 Hz), 7.20 (1H, td, *J* = 8.5, 1.72 Hz), 7.36 (1H, dd, *J* = 8.5, 1.72 Hz), 8.05 (1H, S). ^{13}C NMR (75 MHz, DMSO-d_6, ppm): 52.29 (CH_2), 53.46 (CH_2), 58.39 (CH_2), 59.82 (CH_2), 114.36 (CH), 120.01 (CH), 120.05 (C), 134.41 (CH), 134.44 (CH), 158.77 (CH=N), 163.41 (C).

2.3. X-ray crystallography

A crystal of [Pd(L)Cl] was mounted on a Stoe Image Plate Diffraction system equipped with a ϕ circle goniometer, using Mo-Kα graphite monochromated radiation ($\lambda = 0.71073$ Å) with ϕ range 0-200°. The structure was solved by direct methods using the program SHELXS-97, while the refinement and all further calculations were carried out using SHELXL-97 [31]. The H-atoms were included in calculated positions and treated as riding atoms using the SHELXL default parameters, while the non-H atoms were refined anisotropically using weighted full-matrix least-square on F^2. Crystallographic details are summarized in Table 1. Fig. 1 was drawn with ORTEP [32].

CCDC-1844929 contains the supplementary crystallographic data for this paper. These data can be obtained free of charge at www.ccdc.cam.ac.uk/conts/retrieving.html [or from the Cambridge Crystallographic Data Centre, 12, Union Road, Cambridge CB2 1EZ, UK; fax: (internat.) +44–1223/336-033; E-mail: deposit@ccdc.cam.ac.uk].

Table 1
Crystallographic and structure refinement parameters of [Pd(L)Cl].

	[Pd(L)Cl]
Chemical formula	$C_{11}H_{15}ClN_2O_2Pd$
Formula weight	349.10
Crystal system	monoclinic
Space group	$P\,2_1/a$ (no. 14)
Crystal color & shape	yellow block
Crystal size	0.19 × 0.18 x 0.16
a (Å)	12.4651 (7)
b (Å)	6.4785 (2)
c (Å)	15.8034 (9)
β (°)	93.868 (5)
V (Å^3)	2338.2 (2)
Z	4
T (K)	293 (2)
D_c (g.cm^{-3})	1.821
μ (mm^{-1})	1.658
Scan range (°)	$2.58 < \theta < 28.90$
Unique reflections	3442
Reflections used [$I > 2\sigma(I)$]	2999
R_{int}	0.0303
Final R indices [$I > 2\sigma(I)$][a]	0.0267, wR_2 0.0658
R indices (all data)	0.0337, wR_2 0.0683
Goodness-of-fit	1.037
Max, Min Δρ/e (Å^{-3})	0.560, −0.698

[a] Structures were refined on F_0^2: $wR_2 = [\Sigma[w(F_0^2 - F_c^2)^2]/\Sigma w(F_0^2)^2]^{1/2}$, where $w^{-1} = [\Sigma(F_0^2) + (aP)^2 + bP]$ and $P = [\max(F_0^2, 0) + 2F_c^2]/3$.

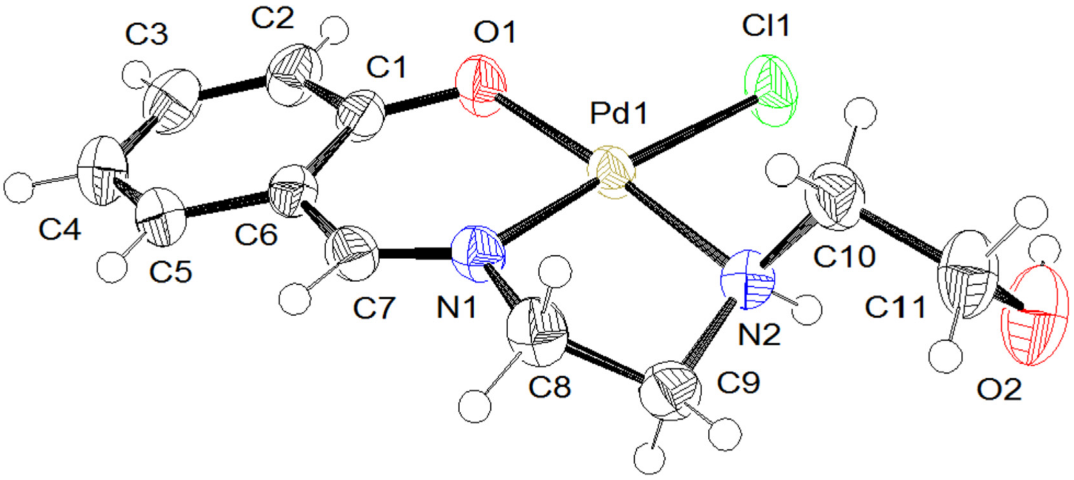

Fig. 1. Ortep drawing of [Pd(L)Cl] at 35% probability level ellipsoids.

2.4. *Computational studies*

Computational investigations were carried out using the Gaussian 09 program package [33]. Geometrical optimization of the [Pd(L)Cl] structure was performed at the B3LYP level using the Density Functional Theory DFT method [34,35]. 6–31++G (d,p) basis set was employed for the C, H, O, N and Cl atoms, and Los Alamos National Laboratory 2-Double-Z (LanL2DZ) [36–38] basis set with effective core potential was assigned for the Pd atom. Further, to ensure that the optimized geometry is the most stable conformation, vibrational frequency calculations were used, and the calculated results showed no imaginary (negative frequencies) eigen values. The vertical electronic excitations on the optimized geometry of [Pd(L)Cl] were performed using the time dependent density functional theory (TDDFT) method [39,40] with the conductor-like polarizable continuum model (C-PCM) [41,42] in ethanol as solvent. Additionally, GaussSum program [43] was used to calculate the percent contribution of different groups to a particular molecular orbital (MO) using the Mulliken population analysis.

3. Results and discussion

3.1. *Structural characterization*

The title complex [Pd(L)Cl] was synthesized in ethanol by the reaction of 2-(2-(2-hydroxyethylamino)ethylimino)methyl phenol (LH) and $PdCl_2$ in the presence of LiCl. A schematic diagram of the complexation is shown in Scheme 1. The complex is air stable at room temperature. The FT-IR study of [Pd(L)Cl] shows strong absorption bands at 1635 and 763 cm^{-1} due to the C=N and C–O groups respectively, confirming the presence of the Schiff base ligand. In the ^1H NMR spectrum, a single peak at 8.05 ppm corresponding to the proton of the azomethine (HC=N) group is observed. Moreover, the four aromatic protons of L appeared between 6.53 and 7.36 ppm. Nevertheless, the molecular structure of the complex was confirmed by single-crystal X-ray structure analysis.

3.2. *Crystal structure*

The molecular structure of [Pd(L)Cl] shows the palladium atom to have an almost perfect square-planar geometry, in which the sum of the angles defining the square being equal to 360° (see Table 2). Moreover, the maximum deviation from the plane defined by Pd, Cl, O1, N1 and N2 (root mean square deviation of fitted atoms = 0.0263) is only 0.0317(9) Å, confirming the high planarity of the complex. This square-planar palladium(II) complex possess similar geometrical parameters to those observed in analogous O,N,N-Schiff base palladium complexes [44–49].

3.3. *Computational investigations and DFT calculations*

Optimization of the palladium complex was carried out in a singlet ground state by DFT method to further understand the electronic structure. All the bond lengths and angles for the complex seems well reproducing the experimental crystal X-ray diffraction structure data. The experimental and calculated geometrical parameters are listed in Table 2.

Contour plots for the selected molecular orbitals (MOs) are depicted in Fig. 2. The calculated MOs energies indicate the chemical stability of the complex. The MOs energies as well as their percent contribution are given in Table 3. The higher energy occupied molecular orbital (HOMO) to the low lying virtual orbital (LUMO) band gab energy is 3.65eV.

Molecular electrostatic potential (MEP) approach is used to assess the reactivity of inorganic and organic molecules as well as the existence of internal and external molecular interactions [50]. As it is observed in Fig. 3, we notice that the electron-rich sites are located on the O–Pd–Cl group while the electrophilic sites are found around the two nitrogen atoms.

Table 2
Selected X-ray and calculated bond distances (Å) and angles (°) of [Pd(L)Cl].

	X-ray	Calc
Bond (Å)		
Pd – N1	1.9586 (18)	2.01115
Pd – N2	2.0516 (19)	2.13577
Pd – O1	1.9912 (16)	2.01231
Pd – Cl	2.3349 (6)	2.35836
Angles (°)		
N1– Pd – N2	84.60 (8)	83.50263
N1– Pd – O1	93.02 (7)	92.42701
N1– Pd – Cl	176.02 (6)	175.06306
N2 – Pd – O1	175.77 (7)	175.68727
N2 – Pd – Cl	91.47 (6)	93.20425
O1 – Pd – Cl	90.88 (5)	90.94852

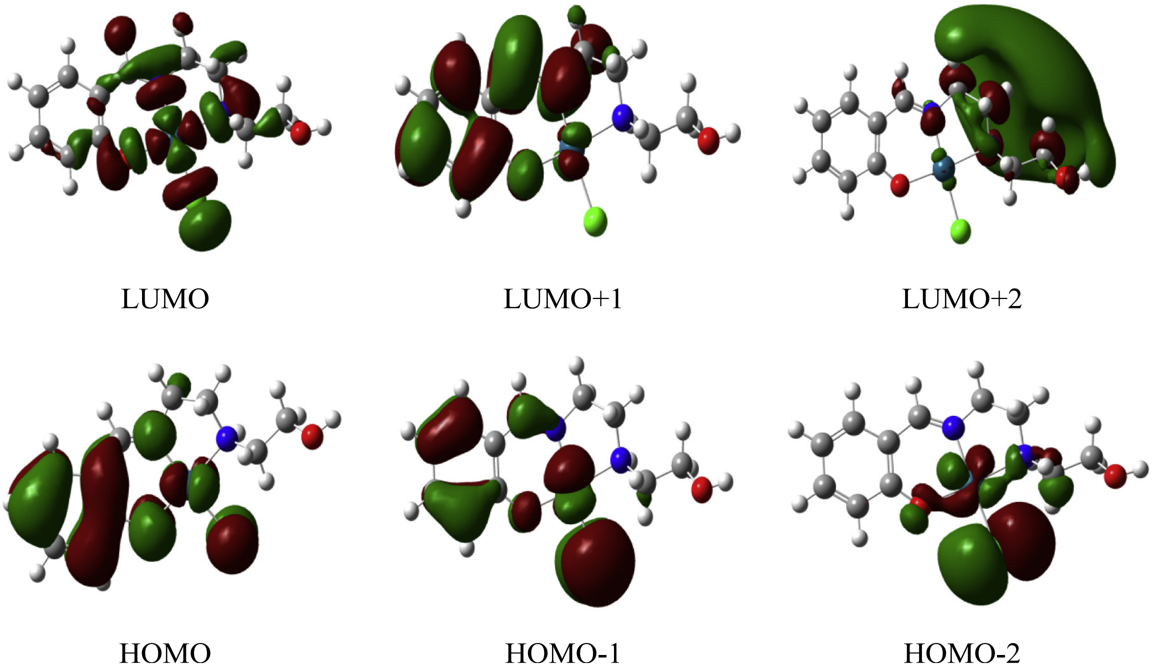

Fig. 2. Contour plots of some selected MOs of [Pd(L)Cl].

Table 3
Energy and composition of some selected molecular orbitals of [Pd(L)Cl].

Mos	Energy (eV)	% of contribution		
		Pd	Ligand (L)	Cl
LUMO+5	0.01	25	75	0
LUMO+4	−0.12	18	82	0
LUMO+3	−0.24	3	97	0
LUMO+2	−0.28	4	96	0
LUMO+1	−1.93	2	98	0
LUMO	−2.23	52	37	12
HOMO	−5.88	11	87	2
HOMO-1	−6.76	36	41	23
HOMO-2	−6.87	81	14	5
HOMO-3	−7.14	27	12	61
HOMO-4	−7.36	9	56	34
HOMO-5	−7.72	73	26	1
HOMO-6	−7.76	12	65	23
HOMO-7	−8.01	2	93	5
HOMO-8	−8.41	26	31	43

3.4. *TDDFT calculation and electronic spectrum*

The UV–vis absorption spectrum of the synthesized complex was measured in ethanol. Several absorption bands were observed in the spectrum of [Pd(L)Cl] as shown in Fig. 4: Low energy broad bands at 285 and 460 nm as well as moderate intensity bands at 305, 340 and 385 nm. Moreover, two intense high-energy bands are observed at 224 and 241 nm respectively.

Therefore, to associate these bands to electronic transitions, the absorption bands of [Pd(L)Cl] were determined by TDDFT. The experimental bands along with the calculated excitation energies, absorption bands, oscillator strengths (f), and MOs transitions configuration are listed in Table 4. The low energy band at 460 nm corresponds to HOMO → LUMO transition ($\lambda_{excitation} = 496$ nm, f = 0.0008) having LMCT (ligand to metal charge transfer) character along with minimal contribution of MXCT (metal to halogen charge transfer) transition. The band at 432 nm ($\lambda_{excitation} = 433$ nm, f = 0.0064) exhibits mixed MLCT (79%) and XMCT (halogen to metal charge transfer, 11%) contributions). The intense high-energy absorptions observed at λ_{max} of 224 nm ($\lambda_{excitation} = 218$ nm, f = 0.3869) and 241 nm ($\lambda_{excitation} = 238$ nm, f = 0.006) have both MLCT and LMCT characters.

3.5. *Electrochemical studies*

Cyclic voltammetry was studied with 4 mM of [Pd(L)Cl] and $PdCl_2$ in distilled water/ethanol (50/50: v/v) mixture with 2 mM nitrate potassium as the supporting electrolyte with a scan rate of 100 mV/s in the potential range −1.5–1.5 V. The obtained cyclic voltammograms are presented in Fig. 5. As it was observed, the $PdCl_2$ shows two peaks, one irreversible cathodic reduction peak at −17 mV and a second quasi-reversible peak with $E_{1/2} = 760$ mV ($\Delta E = 77$ mV). Cyclic voltammograms of [Pd(L)Cl] revealed two peaks with potentials values of 104 and 1150 mV. It is clear that the palladium(II) complex shift the peak potential to positive regions with a large separation of peaks [51]. This displacement is due to the interaction of the metal centre with the environment. The cyclic voltammograms of the palladium(II) complex show quasi-reversible process with a redox complex due to the formation of Pd(II)/Pd(I) couple at $E_{pc} = -950$ mV and $E_{pa} = 104$ mV [52]. The second peak of the complex at 1150 mV is the same as the Pd(II) that is irreversible. This process is due to the electron transfer mechanism, that can be considered as Pd(II)/Pd(III). Furthermore, for better comprehension of the oxidation process, calculations using DFT/B3LYP the Mulliken atomic charges of [Pd(L)Cl] and $[Pd(L)Cl]^+$ were performed (Table 5). The result shows that the chloride atom has a significant enhancement of negative charge, thus the potential peak of the complex is shifted to the positive region, and accordingly, the oxidation is assigned to Pd(II)/Pd(III).

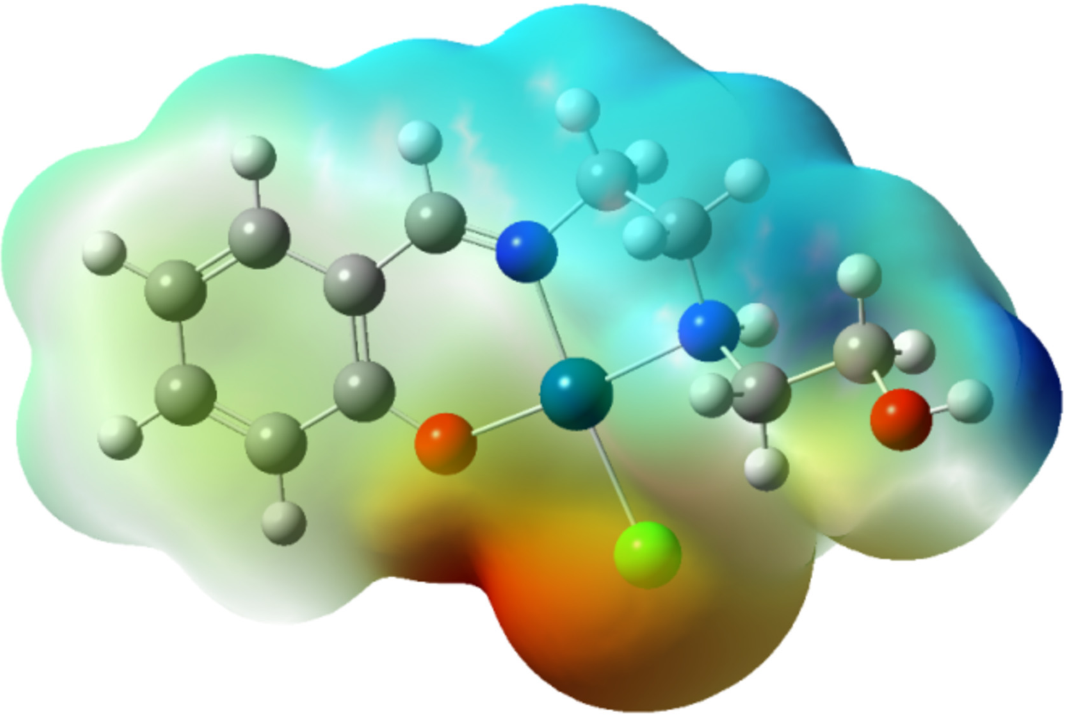

Fig. 3. Molecular electrostatic potential map of [Pd(L)Cl].

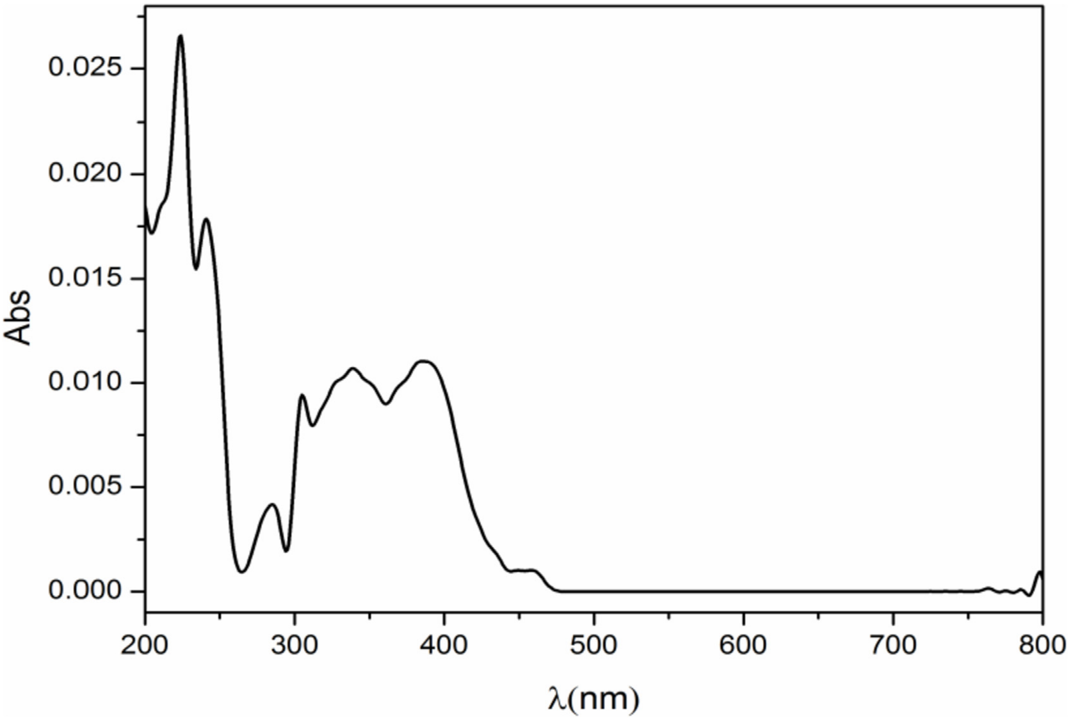

Fig. 4. Experimental UV–Vis spectrum of [Pd(L)Cl] in ethanol.

4. Conclusion

In this work, a new palladium(II) complex [Pd(L)Cl] was synthesized from the Schiff base 2-(2-(2-hydroxyethylamino)ethylimino)methyl phenol (LH) and Li_2PdCl_4. The complex was fully characterized using several techniques including FT-IR, ^{1}H NMR, ^{13}C NMR and ESI-MS. The structure of [Pd(L)Cl] was confirmed by single crystal X-ray structure analysis, thus showing a square-planar complex with a tridentate ligand. Furthermore, it has been shown from cyclic voltammetry technique that the complex exhibit

Table 4
Experimental and calculated electronic transitions by TDDFT/C-PCM method of [Pd(L)Cl] in ethanol.

$E_{\text{excitation}}$ (eV)	λexpt. (nm)	λcalc. (nm)	Osc. Strength (f)	Key transitions	Character
2.49692	460	496	0.0008	HOMO → LUMO (89%)	π(L)→ dπ(Pd) **LMCT**/MXCT
2.85992	432	433	0.0064	HOMO-2 → LUMO (79%)	dπ(Pd) →π(L) **MLCT**/XMCT
3.23812	386	382	0.0085	HOMO-3 → LUMO (75%)	Pπ(Cl) → dπ(Pd) **XMCT**/MLCT
3.36352	340	368	0.0763	HOMO → LUMO+1 (78%)	dπ(Pd) →π(L) **MLCT**
4.22983	305	293	0.1296	HOMO-1 → LUMO+1 (76%)	Pπ(Cl) →π(L) **XLCT**/MLCT
4.53803	285	273	0.1521	HOMO-6 → LUMO (68%)	π(L)→ dπ(Pd) **LMCT**
5.07764	241	238	0.006	HOMO-7 → LUMO (90%)	π(L)→ dπ(Pd) **LMCT**
5.70340	224	218	0.3896	HOMO → LUMO+8 (55%)	dπ(Pd) →π(L) **MLCT**

f = oscillator strength, HOMO = highest occupied molecular orbital, LUMO = lowest unoccupied molecular orbital.

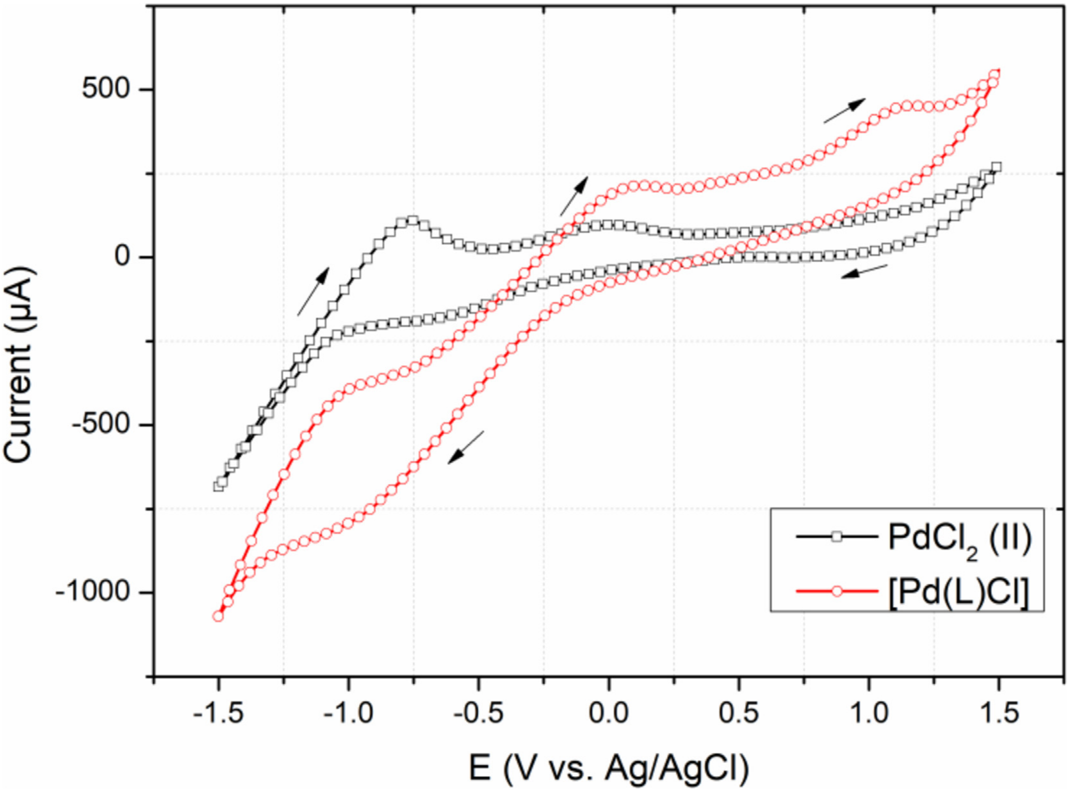

Fig. 5. Cyclic voltammetry of $PdCl_2$ and palladium complex in distilled water/ethanol at 298 K.

Table 5
Mulliken atomic charges of [Pd(L)Cl] and $[Pd(L)Cl]^+$ calculated by DFT/B3LYP.

Atoms	[Pd(L)Cl]	$[Pd(L)Cl]^+$
Pd	0.056151	0.101434
Cl	−0.248118	−0.041918
O	−0.256319	−0.154360
N1	0.004759	−0.020021
N2	−0.536959	−0.545117

a Pd(II)/Pd(III) oxidation process. Calculated vibrational frequencies, electronic spectra and redox properties are in agreement with the experimental findings.

References

[1] L. Yin, J. Liebscher, Carbon – carbon coupling reactions catalyzed by heterogeneous palladium catalysts, Chem. Rev. (2007) 133–173.

[2] K.C. Nicolaou, M.H.D. Postema, C.F. Claiborne, Olefin metathesis in cyclic ether formation. Direct conversion of olefinic esters to cyclic enol ethers with Tebbe-type reagents, J. Am. Chem. Soc. 118 (1996) 1565–1566, https://doi.org/10.1021/ja9534866.

[3] K.C. Nicolaou, T. Montagnon, S.A. Snyder, Tandem reactions, cascade sequences, and biomimetic strategies in total synthesis, Chem. Commun. (2003) 551–564, https://doi.org/10.1039/b209440c.

[4] C. Torborg, J. Huang, T. Schulz, B. Schäffner, A. Zapf, A. Spannenberg, A. Borner, M. Beller, Improved palladium-catalyzed sonogashira coupling reactions of aryl chlorides, Chem. Eur J. 15 (2009) 1329–1336, https://doi.org/10.1002/chem.200802444.

[5] E.M. Beccalli, G. Broggini, A. Fasana, M. Rigamonti, Palladium-catalyzed C-N bond formation via direct C-H bond functionalization. Recent developments in

heterocyclic synthesis, J. Organomet. Chem. 696 (2011) 277–295, https://doi.org/10.1016/j.jorganchem.2010.09.078.

[6] T. Kawamura, N. Matsuo, D. Yamauchi, Y. Tanabe, H. Nemoto, Palladium-catalyzed highly regio- and stereoselective carbon-carbon bond formation reaction of γ-substituted vinylaziridines with a silylated masked acyl cyanide reagent, Tetrahedron 69 (2013) 5331–5341, https://doi.org/10.1016/j.tet.2013.04.129.

[7] G.Y. Li, G. Zheng, A.F. Noonan, Highly active, air-stable versatile palladium catalysts for the C-C, C-N, and C-S bond formations via cross-coupling reactions of aryl chlorides, J. Org. Chem. 66 (2001) 8677–8681, https://doi.org/10.1021/jo010764c.

[8] M.H. Majeed, P. Shayesteh, L.R. Wallenberg, A.R. Persson, N. Johansson, L. Ye, J. Schnadt, O.F. Wendt, Polymer-supported palladium(II) carbene complexes: catalytic activity, recyclability, and selectivity in C–H acetoxylation of arenes, Chem. Eur J. 23 (2017) 8457–8465, https://doi.org/10.1002/chem.201700777.

[9] Y. Li, X. Yu, Y. Wang, H. Fu, X. Zheng, H. Chen, R. Li, Unsymmetrical pincer N-Heterocyclic Carbene–Nitrogen–Phosphine chelated palladium(II) complexes: synthesis, structure, and reactivity in direct csp –H arylation of benzoxazoles, Organometallics 37 (2018) 2–11, https://doi.org/10.1021/acs.organomet.8b00005.

[10] Z. Cimerman, S. Miljanić, N. Galić, Schiff bases derived from aminopyridines as spectrofluorimetric analytical reagents, Croat. Chem. Acta 73 (2000) 81–95.

[11] B. Clarke, N. Clarke, D. Cunningham, T. Higgins, P. McArdle, M. Nı Cholchúin, M. O'Gara, Transition-metal Schiff-base complexes as ligands in tin chemistry. Part 7. Reactions of organotin(IV) Lewis acids with [M(L)]2 [M=Ni, Cu and Zn; H2L=N,N′-bis(3-methoxysalicylidene)benzene-1,3-diamine and its -1,4-diamine analog], J. Organomet. Chem. 559 (1998) 55–64, https://doi.org/10.1016/S0022-328X(98)00417-3.

[12] V. Ambike, S. Adsule, F. Ahmed, Z. Wang, Z. Afrasiabi, E. Sinn, F. Sarkar, S. Padhye, Copper conjugates of nimesulide Schiff bases targeting VEGF, COX and Bcl-2 in pancreatic cancer cells, J. Inorg. Biochem. 101 (2007) 1517–1524, https://doi.org/10.1016/j.jinorgbio.2007.06.028.

[13] A. Shah Zia-ur-Rehman, K.S. Munawar, A.A. Khan, R. Abbasi, M.A. Yameen, A.M. Khan, A.R. Khan, I.Z. Qureshi, H.B. Kraatz, Synthesis, spectroscopic characterization, DFT optimization and biological activities of Schiff bases and their metal (II) complexes, J. Mol. Struct. 1145 (2017) 132–140, https://doi.org/10.1016/j.molstruc.2017.05.098.

[14] A.O. De Souza, F.C.S. Galetti, C.L. Silva, B. Bicalho, M.M. Parma, S.F. Fonseca, A.J. Marsaioli, A.C.L.B. Trindade, R.P.F. Gil, F.S. Bezerra, M. Andrade-Neto, M.C.F. de Oliveira, Antimycobacterial and cytotoxicity activity of synthetic and natural compounds, Quim. Nova 30 (2007) 1563–1566, https://doi.org/10.1590/S0100-40422007000700012.

[15] G. Bringmann, M. Dreyer, J.H. Faber, P.W. Dalsgaard, J.W. Jaroszewski, H. Ndangalasi, F. Mbago, R. Brun, S.B. Christensen, Ancistrotanzanine C and related 5,1‘- and 7,3‘-coupled naphthylisoquinoline alkaloids from ancistrocladus t anzaniensis 1, J. Nat. Prod. 67 (2004) 743–748, https://doi.org/10.1021/np0340549.

[16] Z. Guo, R. Xing, S. Liu, Z. Zhong, X. Ji, L. Wang, P. Li, Antifungal properties of Schiff bases of chitosan, N-substituted chitosan and quaternized chitosan, Carbohydr. Res. 342 (2007) 1329–1332, https://doi.org/10.1016/j.carres.2007.04.006.

[17] J.M. Lazić, L. Vučićević, S. Grgurić-Šipka, K. Janjetović, G.N. Kaluđerović, M. Misirkić, M. Gruden-Pavlović, D. Popadić, R. Paschke, V. Trajković, T.J. Sabo, Synthesis and in vitro anticancer activity of octahedral platinum(IV) complexes with cyclohexyl-functionalized ethylenediamine-N,N′-diacetate-type ligands, ChemMedChem 5 (2010) 881–889, https://doi.org/10.1002/cmdc.201000058.

[18] S.H. Sumrra, M. Ibrahim, S. Ambreen, M. Imran, M. Danish, F.S. Rehmani, Synthesis, spectral characterization, and biological evaluation of transition metal complexes of bidentate N, O donor Schiff bases, Bioinorgan. Chem. Appl. 2014 (2014), https://doi.org/10.1155/2014/812924.

[19] P. Nagababu, J.N.L. Latha, P. Pallavi, S. Harish, S. Satyanarayana, Studies on antimicrobial activity of cobalt(III) ethylenediamine complexes, Can. J. Microbiol. 52 (2006) 1247–1254, https://doi.org/10.1139/w06-087.

[20] A.A. Jarrahpour, M. Motamedifar, K. Pakshir, N. Hadi, M. Zarei, Synthesis of novel azo Schiff bases and their antibacterial and antifungal activities, Molecules 9 (2004) 815–824, https://doi.org/10.3390/91000815.

[21] P.E. Aranha, M.P. dos Santos, S. Romera, E.R. Dockal, Synthesis, characterization, and spectroscopic studies of tetradentate Schiff base chromium(III) complexes, Polyhedron 26 (2007) 1373–1382, https://doi.org/10.1016/j.poly.2006.11.005.

[22] C. Biswas, M.G.B. Drew, E. Ruiz, M. Estrader, C. Diaz, A. Ghosh, Synthesis, crystal structure and magnetic properties of three unprecedented tri-nuclear and one very rare tetra-nuclear copper(ii) Schiff-base complexes supported by mixed azido/phenoxo/nitrato or acetato bridges, Dalton Trans. 39 (2010) 7474, https://doi.org/10.1039/c0dt00331j.

[23] K.C. Gupta, A.K. Sutar, Catalytic activities of Schiff base transition metal complexes, Coord. Chem. Rev. 252 (2008) 1420–1450, https://doi.org/10.1016/j.ccr.2007.09.005.

[24] T.G. Miller, L.J. Theriot, Copper(II) halide complexes with deprotonated N-(2 hydroxyethyl)ethylenediamine, J. Inorg. Nucl. Chem. 38 (1976) 695–697, https://doi.org/10.1016/0022-190(76)80339-9.

[25] G.J. Colpas, B.J. Hamstra, J.W. Kampf, V.L. Pecoraro, Preparation of VO3+and VO2+Complexes using hydrolytically stable, asymmetric ligands derived from Schiff base precursors, Inorg. Chem. 33 (1994) 4669–4675, https://doi.org/10.1021/ic00099a017.

[26] V. Rajendiran, R. Karthik, M. Palaniandavar, H. Stoeckli-Evans, V.S. Periasamy, M.A. Akbarsha, B.S. Srinag, H. Krishnamurthy, Mixed-ligand copper (II)-phenolate complexes: effect of coligand on enhanced DNA and protein binding, DNA cleavage, and anticancer activity, Inorg. Chem. 46 (2007) 8208–8221, https://doi.org/10.1021/ic700755p.

[27] G. Singh, Synthesis and characterization of Si(IV) complexes with tetradentate Schiff base ligands, J. Appl. Chem. 3 (2014) 2176–8221.

[28] A. Mandal, S. Dasgupta, S. Ganguly, A. Bauzá, A. Frontera, D. Das, Cooperative influence of pseudohalides and ligand backbone of Schiff-bases on nuclearity and stereochemistry of cobalt(III) complexes: experimental and theoretical investigation, Dalton Trans. 46 (2017) 15257–15268, https://doi.org/10.1039/c7dt03040a.

[29] M. Hakimi, M. Sarani, Crystal structure of 2-[(2-(2-Hydroxyethylamino) ethylimino) methyl] phenol at 130K, Int. J. Phys. Sci. 7 (2012) 2911–2915.

[30] L. El Firdoussi, A. Baqqa, S. Allaoud, B. Ait Allal, A. Karim, Y. Castanet, A. Mortreux, Selective palladium-catalysed functionalization of limonene: synthetic and mechanistic aspects, J. Mol. Catal. A Chem. 135 (1998) 11–22, https://doi.org/10.1016/S1381-1169(97)00285-9.

[31] G.M. Sheldrick, A short history of SHELX, Acta Crystallogr. Sect. A Found. Crystallogr. 64 (2008) 112–122, https://doi.org/10.1107/S0108767307043930.

[32] L.J. Farrugia, ORTEP -3 for windows - a version of ORTEP -III with a graphical user interface (GUI), J. Appl. Crystallogr. 30 (1997), https://doi.org/10.1107/S0021889897003117, 565–565.

[33] M.J. Frisch, G.W. Trucks, H.B. Schlegel, G.E. Scuseria, M.A. Robb, J.R. Cheeseman, G. Scalmani, V. Barone, B. Mennucci, G.A. Petersson, H. Nakatsuji, M. Caricato, H.P.H.X. Li, A.F. Izmaylov, J. Bloino, G. Zheng, J.L. Sonnenberg, M. Hada, M. Ehara, K. Toyota, R. Fukuda, J. Hasegawa, M. Ishida, T. Nakajima, Y. Honda, O. Kitao, H. Nakai, T. Vreven, J.A.M. Jr., J.E. Peralta, F. Ogliaro, M. Bearpark, J.J. Heyd, E. Brothers, K.N. Kudin, V.N. Staroverov, R. Kobayashi, Normand, J.R. Rendell, K.A.J.C. Burant, S.S. Iyengar, J. Tomasi, M. Cossi, N. Rega, J.M. Millam, M. Klene, J.E. Knox, J.B. Cross, V. Bakken, C. Adamo, J. Jaramillo, R. Gomperts, R.E. Stratmann, O. Yazyev, A.J. Austin, R. Cammi, C. Pomelli, J.W. Ochterski, R.L. Martin, K. Morokuma, V.G. Zakrzewski, G.A. Voth, P. Salvador, J.J. Dannenberg, S. Dapprich, A.D.D.O. Farkas, J.B. Foresman, J.V. Ortiz, J. Cioslowski, D.J. Fox, Fox, Gaussian 09, Revision D.01, Gaussian, Inc., Wallingford CT, 2009. Gaussian 09, Revis. D.01, Gaussian.

[34] A.D. Becke, Density-functional thermochemistry. III. The role of exact exchange, J. Chem. Phys. 98 (1993) 5648–5652, https://doi.org/10.1063/1.464913.

[35] C. Lee, W. Yang, R.G. Parr, Development of the Colle-Salvetti correlation-energy formula into a functional of the electron density, Phys. Rev. B 37 (1988) 785–789, https://doi.org/10.1103/PhysRevB.37.785.

[36] P.J. Hay, W.R. Wadt, Ab initio effective core potentials for molecular calculations. Potentials for the transition metal atoms Sc to Hg, J. Chem. Phys. 82 (1985) 270–283, https://doi.org/10.1063/1.448799.

[37] W.R. Wadt, P.J. Hay, Ab initio effective core potentials for molecular calculations. Potentials for main group elements Na to Bi, J. Chem. Phys. 82 (1985) 284–298, https://doi.org/10.1063/1.448800.

[38] P.J. Hay, W.R. Wadt, Ab initio effective core potentials for molecular calculations. Potentials for K to Au including the outermost core orbitals, J. Chem. Phys. 82 (1985) 299–310, https://doi.org/10.1063/1.448975.

[39] R. Bauernschmitt, R. Ahlrichs, Treatment of electronic excitations within the adiabatic approximation of time dependent density functional theory, Chem. Phys. Lett. 256 (1996) 454–464, https://doi.org/10.1016/0009-2614(96)00440-X.

[40] R.E. Stratmann, G.E. Scuseria, M.J. Frisch, An efficient implementation of time-dependent density-functional theory for the calculation of excitation energies of large molecules, J. Chem. Phys. 109 (1998) 8218–8224, https://doi.org/10.1063/1.477483.

[41] M. Cossi, V. Barone, Time-dependent density functional theory for molecules in liquid solutions, J. Chem. Phys. 115 (2001) 4708–4717, https://doi.org/10.1063/1.1394921.

[42] M. Cossi, N. Rega, G. Scalmani, V. Barone, Energies, structures, and electronic properties of molecules in solution with the C-PCM solvation model, J. Comput. Chem. 24 (2003) 669–681, https://doi.org/10.1002/jcc.10189.

[43] N.M. O'boyle, A.L. Tenderholt, K.M. Langner, cclib: a library for package-independent computational chemistry algorithms, J. Comput. Chem. 29 (2008) 839–845, https://doi.org/10.1002/jcc.20823.

[44] I. Cho, H. Yeo, D. Whang, K. Kim, Structure of chloro[N-(3-dimethylamino-1-propyl)salicylideneaminato]palladium(II), Acta Crystallogr. Sect. C Cryst. Struct. Commun. 48 (1992) 1488–1489, https://doi.org/10.1107/S0108270192002543.

[45] J.H. Lee, S.M. Lee, S.W. Lee, Synthesis and structures of a palladium macrocycle, a six-membered palladacycle, and a palladium compartment complexes: [Pd(L1)Cl],[Pd(NH2CH2CH2CH2NH2)Cl2], and [Pd(L2)] (HL1=(E)-2)(((3aminopropyl)imino)methyl)-6-methoxyphenol; H2L2=N,N′-bis(3-methoxys, Polyhedron 119 (2016) 120–126, https://doi.org/10.1016/j.poly.2016.08.039.

[46] D. Das, P. Maiti, A. Kr, Notes Synthesis, Structure and Catalytic Aspects of the Palladium (II) Complex [PdLCl] (where LH = 2-formyl-4-methyl-6-N-Ethylpiperidineiminomethylphenol), vol. 52, 2013, pp. 863–867.

[47] P. Liu, X.-J. Feng, R. He, Salen and half-salen palladium(II) complexes:

synthesis, characteriztion and catalytic activity toward Suzuki–Miyaura reaction, Tetrahedron 66 (2010) 631–636, https://doi.org/10.1016/j.tet.2009.11.072.

[48] W.B. Cross, E.G. Hope, G. Forrest, K. Singh, G.A. Solan, N-Triisopropylphenyl-substituted N,Npy, O pincers as supports for mononuclear palladium(II) complexes and hydrogen-bonded dimeric assemblies, Polyhedron 59 (2013) 124–132, https://doi.org/10.1016/j.poly.2013.04.049.

[49] L.A. Wright, E.G. Hope, G.A. Solan, W.B. Cross, K. Singh, O, N,N-Pincer ligand effects on oxidatively induced carbon–chlorine coupling reactions at palladium, Dalton Trans. 44 (2015) 6040–6051, https://doi.org/10.1039/C5DT00062A.

[50] P. Politzer, D.G. Truhlar, Chemical Applications of Atomic and Molecular Electrostatic Potentials, Springer US, Boston, MA, 1981, https://doi.org/10.1007/978-1-4757-9634-6.

[51] M. Aslantaş, E. Kendi, N. Demir, A.E. Şabik, M. Tümer, M. Kertmen, Synthesis, spectroscopic, structural characterization, electrochemical and antimicrobial activity studies of the Schiff base ligand and its transition metal complexes, Spectrochim. Acta Part A Mol. Biomol. Spectrosc 74 (2009) 617–624, https://doi.org/10.1016/j.saa.2009.07.006.

[52] B. Shafaatian, A. Soleymanpour, N. Kholghi Oskouei, B. Notash, S.A. Rezvani, Synthesis, crystal structure, fluorescence and electrochemical studies of a new tridentate Schiff base ligand and its nickel(II) and palladium(II) complexes, Spectrochim. Acta Part A Mol. Biomol. Spectrosc 128 (2014) 363–369, https://doi.org/10.1016/j.saa.2014.02.179.